Arctic Ocean in CMIP6 Models: Historical and projected temperature and salinity in the deep basins

Narges Khosravi[1], Qiang Wang[1], Nikolay Koldunov [2,1], Claudia Hinrichs [1], Tido Semmler [1], Sergey Danilov [1], Thomas Jung [1,3]

[1]Alfred Wegener Institute, Helmholtz Centre for Polar and Marine Research, Bremerhaven, Germany
[2]MARUM—Center for Marine Environmental Sciences, Bremen, Germany
[3]Department of Physics and Electrical Engineering, University of Bremen, Bremen, Germany

Key Points:

- The issue of too deep and too thick Arctic Atlantic Water layer continues to be present in Coupled Model Intercomparison Project 6
- On average the Arctic Ocean is subject to a much stronger warming than the global mean in a warming climate
- The upper ocean salinity decreases in the future in the multi-model mean, but not in all individual models

Corresponding author: Narges Khosravi, narges.khosravi@awi.de

Corresponding author: Qiang Wang, Qiang.Wang@awi.de

Abstract

We examine the historical and projected hydrography in the deep basin of the Arctic Ocean in 23 climate models participating in the sixth phase of the Coupled Model Intercomparison Project (CMIP6). The comparison between historical simulations and observational climatology shows that the simulated Atlantic Water (AW) layer is too deep and too thick among the majority of the models and in the multi-model mean (MMM). Moreover, the halocline is too fresh in the MMM. These issues indicate that there is no visible improvement in the representation of Arctic hydrography in the CMIP6 compared to the CMIP5. The climate projections reveal that the sub-Arctic seas are outstanding warming hotspots, supplying a strong warming trend in the Arctic AW layer. The MMM temperature increase averaged in the upper 700 m till the end of the 21st century in the Arctic Ocean is about 40% and 60% higher than the global mean in the SSP245 and SSP585 scenarios, respectively. Comparing the AW temperature in the present day with its future change among the models shows that the temperature climate change signals are not sensitive to the model biases in the present-day simulations. The upper-ocean salinity is projected to become fresher in the Arctic deep basin in the MMM. However, the salinity spread is rather large and the tendency toward stronger upper ocean stratification in the MMM is not shared among all the models. The identified hydrography biases and spread call for a collective effort for systematic improvements of coupled model simulations.

Plain Language Summary

Coupled climate models, which include atmosphere, ocean, land and ice components, are crucial tools for understanding and projecting climate change, especially for the Arctic which is undergoing unprecedented changes. The Arctic Ocean has a strong halocline that separates the warm Atlantic water in the mid-layer from the sea-ice at the surface and so prevents melting from below. However, a weakening of the Arctic Ocean stratification (Atlantification) might cause significant sea ice basal melting and accelerate sea ice decline. We examined the simulated temperature and salinity in the Arctic Ocean deep basin in the most recent state-of-the-art climate models providing information for the next IPCC Assessment Report. We found that the representation of Arctic temperature and salinity has not improved much in the new generation of climate models compared to the last generation. Moreover, the Arctic Ocean is subject to a much stronger warming than the average global ocean under climate change. However, because of considerable spread in the upper-ocean salinity simulation the models do not agree on whether future changes in stratification will facilitate upward heat fluxes from the Atlantic water layer to the base of sea ice. For accurate predictions, current coupled climate models have to be further improved.

1 Introduction

The Arctic is an integral part of the climate system that has undergone dramatic changes in recent decades. This includes the so-called Arctic amplification, which refers to atmospheric temperature increase in the Arctic that is much higher than global mean values (Serreze & Francis, 2006), and that is associated with a rapid decrease in sea ice area and volume (Johannessen et al., 2004; Serreze & Stroeve, 2015; Notz & Stroeve, 2016; Dai et al., 2019). Like the atmosphere, the interior of the Arctic Ocean is also experiencing significant changes. Observations show an increase in the temperature of the Atlantic Water (AW) layer that occupies the intermediate depth of the Arctic Ocean (Polyakov et al., 2005; Dmitrenko et al., 2008). Despite a strong freshening and thickening of the halocline in the western Arctic in recent decades (Giles et al., 2012; Wang et al., 2016a; Proshutinsky et al., 2019), the isolation of the surface ocean and sea ice from warm AW

is found to become weaker in the eastern Arctic (Polyakov et al., 2010; Ivanov et al., 2016); the latter process is commonly referred to as Arctic Atlantification (Polyakov et al., 2017).

To better understand these changes and provide trustworthy future projections, high-quality modelling of the Arctic Ocean, including the proper representation of the main processes, such as water mass transformations and development of the Arctic Atlantification is required. This is especially important because of the limited amount of observational data from the Arctic, due to its remoteness, harsh environmental conditions, sea ice cover, and limited solar illumination that allow only restricted use of satellites to monitor ocean properties.

AW is the main oceanic heat source of the Arctic deep basin (Rudels & Friedrich, 2000). The warm AW layer is characterized by high temperatures and salinity in comparison to the halocline water, and has potential impacts on the sea ice cover (Carmack et al., 2015; Dmitrenko et al., 2014; Polyakov et al., 2010). The AW inflow from the Nordic Seas consists of two branches: One through the Fram Strait, i.e. the West Spitsbergen Current, and the second one through the Barents Sea. Observations show that the Barents Sea branch loses most of its heat to the atmosphere already in the Barents Sea, while the Fram Strait branch is the major heat source of the Arctic AW layer (Smedsrud et al., 2013; Schauer et al., 2008). Part of the AW at the Fram Strait recirculates southwards into the Greenland Sea (Marnela et al., 2013). It has been shown that the water mass properties at the Fram Strait as well as the partition of the West Spitsbergen Current into the Arctic interior can be significantly influenced by mesoscale eddies (Hattermann et al., 2016; Wekerle et al., 2017).

As the baroclinic Rossby radius in the Arctic Ocean is on the order of a few kilometres or less, even state-of-the-art ocean models used in climate simulations are too coarse to resolve mesoscale eddies. Although model developers tune their model parameterizations and parameters to improve the representation of the ocean circulation in the Arctic region, significant temperature and salinity biases still exist as shown in previous model intercomparison studies (Holloway et al., 2007; Proshutinsky & Kowalik, 2007; Proshutinsky et al., 2016; Wang et al., 2016a, 2016b; Ilıcak et al., 2016). In particular, both the ocean models analyzed in the Arctic Ocean Model Intercomparison Project (AOMIP) and the ocean components of global climate models analyzed in the Coordinated Ocean Ice Reference Experiments phase 2 (COREII) project, when driven by atmospheric reanalysis forcing, show a large model spread in their simulated temperature and salinity in the Arctic halocline and AW layer (Holloway et al., 2007; Ilıcak et al., 2016; Wang et al., 2016b).

The Coupled Model Intercomparison Project (CMIP) was initiated by the World Climate Research Programme to provide a standardized framework for carrying out climate change experiments with fully coupled models (Meehl et al., 2000). Although the fifth phase of CMIP (CMIP5) incorporated many of the same ocean models as those assessed in the COREII project (in ocean stand-alone simulations, (Ilıcak et al., 2016)), the model spread of Arctic Ocean temperature and salinity in CMIP5 models is significantly larger than in COREII models (Shu et al., 2019). The most probable explanation for this finding is that fully coupled models are further influenced by bias in atmospheric and land models as well as by biases that are amplified through two-way coupling between the ocean and the atmosphere, which is absent from ocean-only experiments. One major common issue in both forced ocean simulations and CMIP5 coupled model simulations is that the Arctic AW layer is too deep and too thick as reported in the aforementioned model assessment studies.

Currently, CMIP is in its sixth phase (CMIP6, (Eyring et al., 2016)) and it is crucial to analyse the performance of these models in simulating the present and the future state of temperature and salinity in the halocline and AW layer in the Arctic deep basin. Here, we examine the historical simulations and the future projections in CMIP6 cou-

pled models. As a first step in assessing the ability of the CMIP6 models in representing the Arctic Ocean, in this paper, we focus on the following questions: (1) Can the available CMIP6 models adequately reproduce the temperature and salinity in the Arctic deep basin? Specifically, we want to know whether the large temperature and salinity biases in the Arctic deep basin found in CMIP5 models are reduced in the CMIP6 models. (2) How will Arctic hydrography develop and how does the warming trend in the Arctic Ocean deep basin compare to the global mean trend in the future warming climate? It should be mentioned that many modelling groups still had not uploaded all their CMIP6 results at the time of writing this paper. However, a timely assessment of currently available CMIP6 results at the current stage is required not least because many modelling groups have already started planning their model configurations for the next phase of CMIP.

This paper is organized as follows: Data processing and methodology are described in section 2. Subsequently, the results and discussion are presented in sections 3 and 4 respectively, followed by conclusions and suggestions for further investigations in section 5.

2 Methodology and Data

We assess the temperature and salinity in the CMIP6 historical simulations against the Polar Science Center Hydrographic Climatology (PHC) 3.0 database (Steele et al., 2001). The mean vertical distribution of temperature and salinity in the Eurasian and Canadian basins are evaluated separately. These are the deep ocean basins with bottom topography deeper than 300 m and separated by the Lomonosov Ridge. For the sake of simplicity we will refer to the climatological mean as climatology hereafter which is calculated over 36 years (1979-2014) of the historical experiments. Moreover, to assess the future change of the Arctic Ocean, the climate change signals of the temperature and salinity are calculated by taking the difference between the present day and long-term future values. Here we chose the definitions of present day (1995-2014) and long-term future (2081-2100) according to the time intervals that are planned to be used in the upcoming IPCC AR6 definitions. Two Shared Socioeconomic Pathways (SSP) scenarios (O'Neill et al., 2016) are assessed in this study: SSP245 (the so-called medium forcing scenario with 4.5 W/m2 forcing at the end of the century) and SSP585 (the "high-end" of carbon emission or the strong forcing scenario with high carbon emission for radiative forcing of 8.5 W/m2 by 2100). The future changes in temperature and salinity in the Arctic deep basin are also compared to the global mean changes.

The CMIP6 model data is provided through the Earth System Grid Federation (ESGF). The CMIP6 historical experiments cover the time period from 1850 to 2014. The projections from 2015 to 2100 are carried out as part of the scenario experiments, which define future scenarios based on approximate total radiative forcing levels by 2100. Among the many models participating in CMIP6, only 23 models from 18 institutions (see Table 1) have already provided the required data from both their historical and SSP experiments. Because there are different numbers of ensemble realizations available for different models and experiments, we only use the first ensemble member (r1i1p1f1) for each model and experiment as done in the previous CMIP5 assessment (Shu et al., 2019).

The models have different grid resolutions and provide their three-dimensional data (here sea-water potential temperature and salinity) on different depth levels. Before computing the multi-model mean (MMM), all model outputs were re-gridded to the common grid of PHC3.0 climatological data ($1\times1^\circ$) for the corresponding variable using Climate Data Operator (CDO) (Schulzweida, 2019). Then, the re-gridded data were used to produce the MMM fields. Likewise, when averaging over a vertical level was needed, the individual model levels were interpolated to the 33 levels of the PHC3.0 data. However, given that individual models have different grid structures and topographies, re-gridding them to the $1\times1^\circ$ grid causes imperfections over continental slopes when cal-

Table 1: The models for which data were made available (as of September 2020) on the Earth System Grid Federation server (`https://esgf-data.dkrz.de/projects/esgf-dkrz/`) for both historical and two selected scenario experiments (SSP245 and SSP585) of the following variables: potential temperature and salinity. KPP- k-profile parameterization by Large et al. (1994), TKE - Turbulent Kinetic Energy scheme based on the model of Gaspar et al. (1990), CTC - Turbulence closure scheme based on Canuto et al. (2001, 2002), EPBL - Energetically constrained parameterization of the surface boundary layer (Reichl & Hallberg, 2018), PP - Richardson number-dependent scheme of Pacanowski and Philander (1981), NK - surface mixed layer parameterization of Noh and Jin Kim (1999). GLS - generic length scale scheme of Umlauf and Burchard (2003).

No.	Model Name	Institution ID	Grid Resolution (lon × lat)	Number of levels	Mixing scheme
1	ACCESS-CM2	CSIRO-ARCCSS	360 × 300	50	KPP
2	ACCESS-ESM1-5	CSIRO-ARCCSS	360 × 300	50	KPP
3	AWI-CM-1-1-MR	AWI	Unstructured grid ca. 25 km res	46	KPP
4	BCC-CSM2-MR	BCC	360 × 232	40	KPP
5	CAMS-CSM1-0	CAMS	360 × 200	50	KPP
6	CanESM5	CCCma	360 × 291	45	TKE
7	CESM2	NCAR	320 × 384	60	KPP
8	CESM2-WACCM	NCAR	320 × 384	60	KPP
9	CIESM	THU	384 × 320	60	KPP
10	CMCC-CM2-SR5	CMCC	363 × 292	50	TKE
11	EC-Earth3	EC-Earth-Consortium	362 × 292	75	TKE
12	EC-Earth3-Veg	EC-Earth-Consortium	362 × 292	75	TKE
13	FGOALS-g3	CAS	360 × 218	30	CTC
14	CGDL-CM4	NOAA-GFDL	1440 × 1080	35	EPBL
15	CGDL-ESM4	NOAA-GFDL	720 × 576	35	EPBL
16	INM-CM4-8	INM	360 × 180	33	PP
17	INM-CM5-0	INM	360 × 180	33	PP
18	IPSL-CM6A-LR	IPSL	363 × 332	75	TKE
19	MIROC6	MIROC	360 × 256	63	NK
20	MPI-ESM1-2-HR	MPI-M	802 × 404	40	PP
21	MPI-ESM1-2-HR	MPI-M	256 × 220	40	PP
22	MRI-ESM2-0	MRI	360 × 363	61	GLS
23	NESM3	NUIST	362 × 292	46	TKE

culating the MMM (as indicated by grid scale noise). None of the aspects mentioned above is expected to impact the conclusions of this study.

For each model, the Atlantic Water Core Temperature (AWCT) is determined by finding the maximum temperature along the vertical axis at each location. The depth at which the maximum temperature occurs is defined as the Atlantic Water Core Depth (AWCD). In order to eliminate outlier results and for the outcome to be comparable to the assessment of CMIP5 AW layer, we implemented the same criterion as Shu et al. (2019) when calculating MMM. That is, if the simulated AWCD in any of the two basins is deeper than four times that of the observation, then the model is not considered in the MMM calculation (see Figure 2).

3 Results

3.1 Model evaluation from historical simulations

The vertical profiles of observed hydrography highlight the vertical structure of the Arctic Ocean water mass in the Eurasian and Canadian basins (Figure 1). Averaged over each basin, the halocline is located above about 200m and 300m in the Eurasian and Canadian basins, respectively. Below the cold halocline the warm AW layer can be found, which occupies the layer between the halocline and about 800 m depth (as indicated by the depth of 0°). The mean AWCT is about 1° and 0.5°C and the mean AWCD amounts to about 300m and 500m in the Eurasian and Canadian basins, respectively. Although the MMM reproduces the main vertical structure of the temperature and salinity to some extent, there are substantial biases. More specifically, the simulated MMM AWCD is about 250m deeper than observed; and the simulated AW layer is too thick with its lower boundary reaching to a depth of about 3000m, instead of about 800m in the observation (Figure 1a). This is very similar to the results of CMIP5 models (Shu et al., 2019).

Inspection of individual models reveals that most of the models overestimate the AWCD (Figure 2a). There are three models with AWCD similar to or smaller than the observations in either basin; however, their AWCT is much lower than observed (Figure 2b). In particular, four models have extremely deep AW in at least one of the basins (depicted with white color in Figure 2a), so they are excluded when calculating the MMM as described in Section 2. Even with these models excluded, the model spread (defined by the standard deviation; std) of the AWCD is as large as about 250m in both basins (Figure 2a). The model spread of the AWCT is also quite pronounced in both basins (about 1°C, Figure 2b). Note, that the range (difference between the maximum and the minimum) of AWCT in the models is more than 3.5°C in both basins. It is also worth noting, that the AWCD and AWCT biases are very similar in the two basins for all models, which may not be too surprising given that the Canadian basin lies "downstream" of the Eurasian one (see below). The vertical transects of temperature along the AW pathway in individual models further illustrate the model biases and spread (Figure S2).

The spatial patterns of the MMM AWCT and AWCD are compared to observational estimates in Figure 3. The observations clearly show the AW pathway: AW enters the Arctic Ocean through the Fram Strait and circulates cyclonically along the continental slope in the Eurasian Basin, it then penetrates into the Canadian Basin in a cyclonic direction. The AWCD deepens along the AW pathway, and it is on average about 200m deeper in the Canadian Basin than in the Eurasian Basin (see also Figure 1a and Figure 2a). The MMM AWCT is colder than the observed nearly everywhere inside the Arctic Ocean; although its spatial pattern indicates that, on average, the simulated AW circulation is cyclonic as expected. The MMM AWCD reproduces the contrast between the two deep basins (deeper in the Canadian Basin); however, AWCD is overestimated by models in both basins. There are differences in the detailed spatial pattern of AWCD between the MMM and the observation. One outstanding difference is that the observed maximum is in the southeastern Canadian Basin, whereas in the MMM it is located in the western Canadian Basin.

The simulated salinity also has large biases in both basins, which are most pronounced in the halocline and at the surface (Figure 1b). The MMM salinity has negative biases up to 0.5 psu in the halocline in the Canadian Basin, and even larger biases in the Eurasian Basin. The largest fresh bias is closer to the surface in the Eurasian basin than in the Canadian Basin given that the halocline is thinner in the Eurasian Basin. At the surface, the MMM salinity bias is negative in the Eurasian Basin and slightly positive in the Canadian Basin. Inspecting individual models reveals that the models have a large spread in the simulated salinity in the upper ocean. The largest spread is at the surface, with the difference between the maximum and minimum surface salinity reaching more than 5 psu. Even at 200 m depth, the range of the simulated salinity between the mod-

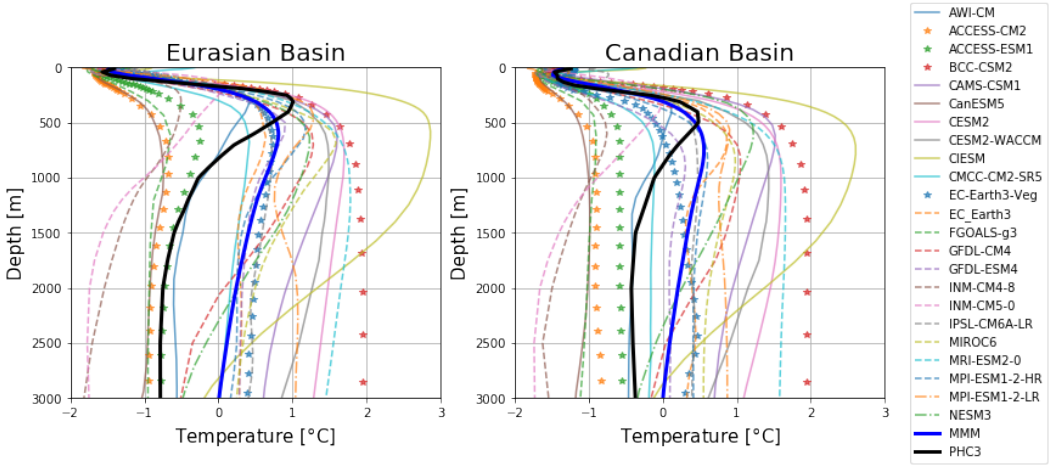

(a)

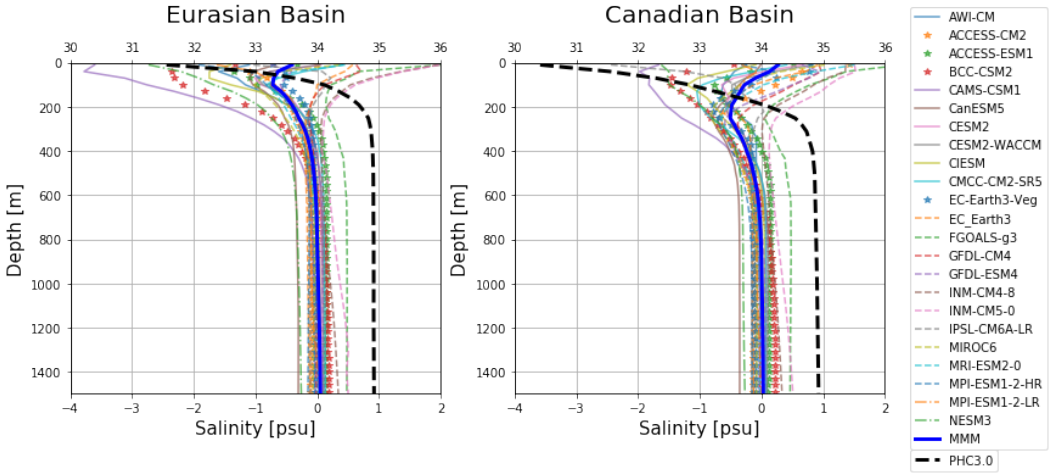

(b)

Figure 1: Climatological (1979-2014) and basin mean potential temperature (top) and salinity (bottom) in the Arctic Ocean. The Eurasian basin is shown on the left and Canadian basin on the right panels. The 19 models, which are taken into account for generating the multi-model means (MMM), are shown as thin solid and dashed lines. The four models excluded from the MMM are marked differently (with a star). For temperature profiles the thick blue and black curves represent the MMM and the PHC3.0 climatology, respectively. Note that salinity profiles are presented as biases with respect to the PHC3.0 climatology; The black dashed curve represents the PHC3.0 observation and the thick blue curve is the MMM bias. The original salinity profiles are shown in Figure S1.

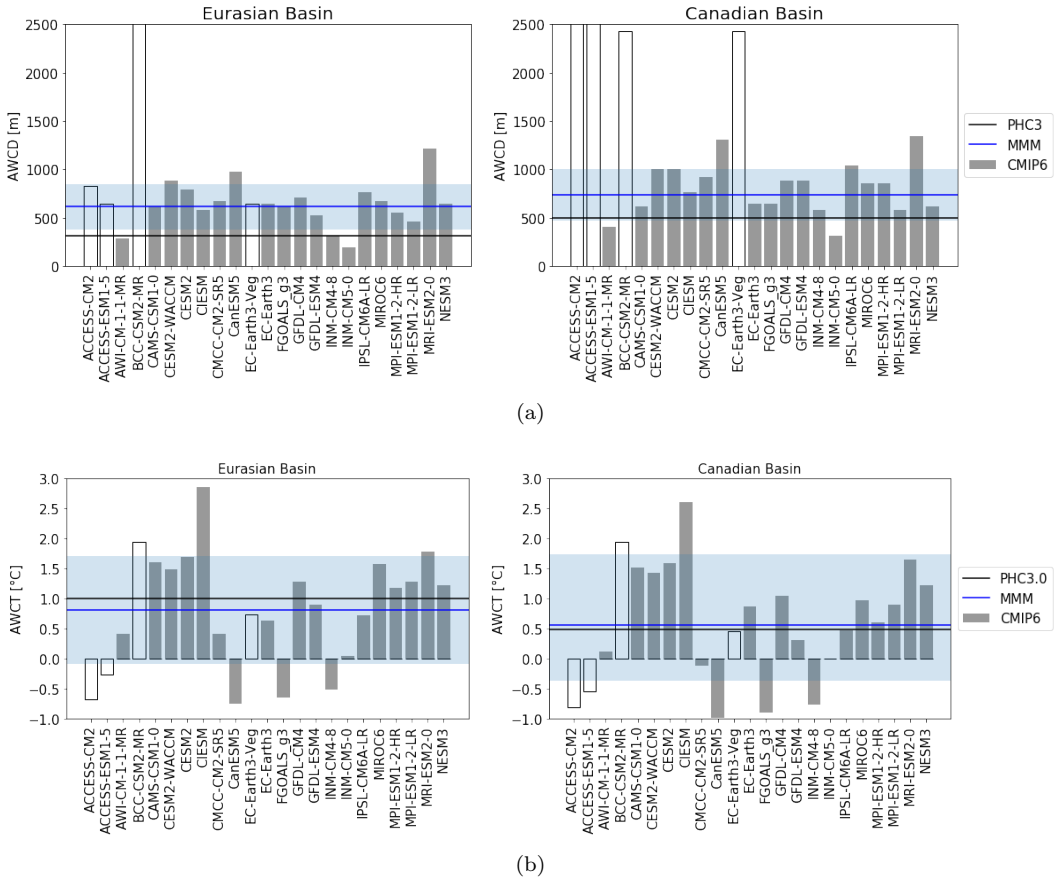

Figure 2: Atlantic Water core depth (AWCD, in m) and Atlantic Water core temperature (AWCT, in °C) from the individual CMIP6 models (bars), multi-model-mean (blue solid line) and PHC3.0 climatology (black solid line) for the Eurasian and Canadian basins. White bars represent models that have been discarded from further analysis (i.e. models with AWCD larger than 4 times that of the observation). The models shown with white bars are excluded in the multi-model mean. The multi-model mean ± one standard deviation is indicated through light blue shading.

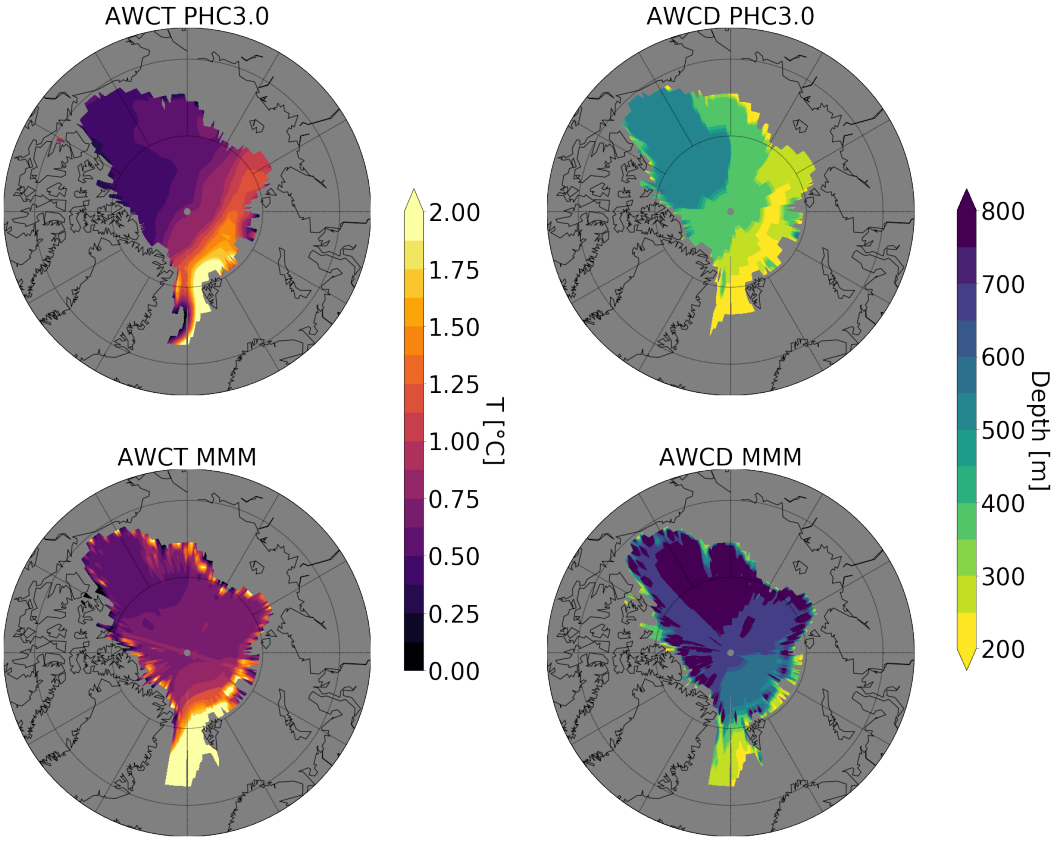

Figure 3: The climatological mean of the Atlantic water core temperature (AWCT in °C) and Atlantic water core depth (AWCD in m) from PHC3.0 and the MMM of 19 CMIP6 models (historical experiment; 1979-2014).

els is still more than 1 psu. Although the MMM underestimates the upper ocean salinity on average (thus overestimating the Arctic freshwater content), some models do significantly overestimate the upper ocean salinity.

Upper ocean salinity in model simulations can be significantly influenced by vertical mixing coefficients (Zhang & Steele, 2007), so different vertical mixing parameterizations and different levels of numerical vertical mixing between the models can explain part of the model spread in salinity. Among other factors, Arctic freshwater sources, including river runoff and precipitation, which typically have considerable spread in climate model simulations (Shu et al., 2018), can also contribute to the identified model spread in upper ocean salinity. The largest MMM salinity bias is in the mid to lower halocline, so on average it is possibly more related to vertical mixing in the ocean.

In summary, CMIP6 historical simulations show a too deep and too thick AW layer and a too fresh halocline in a MMM sense, and they show considerable model spread in the simulated temperature and salinity. These issues are the same as in CMIP5 models (Shu et al., 2019). Importantly, not only these "high-level" issues can be found in CMIP5 and CMIP6 models; also some details, such as the location of maximum AWCD (Figure 3) and opposite biases in MMM sea surface salinity between the two basins (Figure 1b), are essentially the same in the two generations of CMIP models. Therefore, for the representation of the Arctic hydrography, CMIP6 does not show clear improvements compared to CMIP5.

3.2 Climate change projections

In this section, we will explore the climate change signals of Arctic temperature and salinity for the two scenarios (i.e. ssp245 and ssp585). Climate change for zonal mean temperature in the Arctic deep basins as simulated by CMIP6 models is presented in Figure 4. In both scenarios, ocean warming mainly occurs in the upper 2000 m. This holds for MMM as well as most individual models. For both basins and scenarios the strongest warming signal for MMM is found in two depth ranges – that is at depths close to the observed AWCD (about 200-500 m depth) and at the surface. The former indicates the warming of the AW layer, while the latter reflects the surface warming associated with atmospheric warming. In both scenarios, the warming in the AW layer is stronger in the Eurasian Basin than in the Canadian Basin. This is consistent with the fact that the AW circulates cyclonically from the Eurasian Basin to the Canadian Basin. For MMM the maximum climate change signal for the AW temperature amounts to about 1.7°C (1.4°C) in the Eurasian (Canadian) Basin in SSP245, while it is about 3°C and 2.4°C in the two basins in SSP585, respectively. At the surface, the climate change signals in the two basins are comparable. In fact, the MMM surface temperature climate change amounts to about 1° and 2.8° in the SSP245 and SSP585 scenarios, respectively. Only in the Canadian Basin and for the more extreme SSP585 scenario is projected climate change in surface temperature larger than in the AW layer (by up to about 0.4°C). As the strongest warming in the AW layer is at depth shallower than the simulated AWCD in historical simulations (cf. Figure 1b and Figure 4), the AWCD becomes shallower at the end of the 21st century (by about 200 m in both warming scenarios, see Figure. S3).

The spatial patterns of MMM climate change signals for AWCT are consistent with the source and circulation direction of AW (Figure 5). In both scenarios the strongest warming signal starts at the Fram Strait, the entrance of the warm AW; it then propagates into and around the Eurasian Basin and then Canadian Basin. The warming at the Fram Strait amounts to more than 2°C and 4°C in the SSP245 and SSP585 scenarios, respectively. The warming signal does not propagate from the Eurasian Basin to the Canadian Basin in a strictly cyclonic direction along the boundary of the deep basins (anticipated from existing knowledge of the Arctic ocean circulation), as indicated by the extension of the warming signal from the Eurasian Basin toward the Canadian Basin through the central Arctic. As the model resolutions in CMIP6 models are typically quite coarse, the associated numerical diffusion is most probably the main reason for such a spatially diffused pattern of anthropogenic warming in the central Arctic ocean.

Despite the large warming trend in the MMM, the individual models show a large spread of the climate change signals for temperature. Not all the temperature climate change signals from individual models are physically consistent with those of the MMM (Figure 4, for model spread see also the Hovmöller diagrams of temperature for individual models in Figure S4). The range of temperature climate change signals among the models is about 4°C in SSP245 and 7°C in SSP585; this is more than twice of the MMM climate change signals. There are even two models with negligible or even negative temperature changes in the core depth range of the AW layer in both scenarios, while all other models predict ocean warming in the AW layer. Furthermore, the models do not agree on whether the ocean surface or the AW layer will warm more in the future. In both basins and in both scenarios, there are models with relatively stronger warming at the surface and models with stronger warming in the AW layer.

To compare the extent of projected warming in the Arctic deep basin with the projected global mean warming, Hovmöller diagrams for MMM temperature for these two ocean areas are shown in Figure 6a. In the Arctic Ocean, the strongest warming trend can be seen at the depth where AW prevails, while the surface ocean shows a comparatively smaller warming trend, as can be seen in Figure 4. In contrast, the maximum global average warming trend is at the ocean surface. Although the global mean surface warming trend is stronger than the mean over the Arctic surface, the warming in the AW layer

of the Arctic Ocean causes stronger overall warming in the Arctic deep basin, as indicated by the time series of mean temperature averaged over the upper 700 m and upper 2000 m (Figure 6b). The increase in temperature averaged over the upper 700 m of the Arctic deep basin at the end of the 21 century is higher than that of the global ocean by 0.4° (40%) and 1° (60%) in the SSP245 and SSP585 scenarios, respectively. Although the amplitude of the temperature increase averaged over the upper 2000 m is smaller than averaged over the upper 700 m, the amplified warming in the Arctic deep basin is more pronounced. It is about 75% higher in the Arctic deep basin than in the global deep basin at the end of the 21st century in the SSP585 scenario. If we consider the whole Arctic Ocean including continental shelves, we get a similar conclusion, that is the Arctic Ocean is subjected to a stronger warming than the global ocean on average (Figure S5). It is worth stressing that the warming in the Arctic Ocean has just started to be significant from the 2020s according to the MMM; in contrast the temperature change is rather small from the beginning of the industrialization to the present day (see the Hovmöller diagram for Arctic temperature covering the whole CMIP historical simulation period in Figure S6).

The MMM salinity climate change signals for both basins show a freshening of the upper ocean in both scenarios (Figure 9). The strongest freshening occurs in the upper halocline and in the mixed layer (upper 200 m), indicating an increase in freshwater storage in the Arctic Ocean in the future. The freshening is consistent with an enhanced hydrological cycle, and thus increased freshwater supply to the Arctic Ocean in a warming climate (Carmack et al., 2015; Shu et al., 2018). The freshening is stronger in the Canadian Basin than in the Eurasian Basin, quite possibly due to changes in the ocean surface stress induced by sea ice decline (Wang et al., 2019). On average the surface Ekman transport is directed from the Eurasian Basin toward the Canadian Basin. Sea ice decline increases ocean surface stress, thus the Ekman transport, which enhances freshwater accumulation in the Canadian Basin and tends to reduce it in the Eurasian Basin (Wang et al., 2019).

Although salinity for MMM shows freshening in the Arctic Ocean in both warming scenarios, some of the models predict an increase of salinity in the upper ocean, either near the surface or in the halocline (Figure 6). The range of projected salinity changes among the models amount to about 2-3 psu even when the "outlier models" are excluded, much larger than the MMM salinity climate change signal. The large model spread in the simulated salinity in the future scenarios implies large spread in the simulated future Arctic freshwater storage in CMIP6 models. Therefore, the issue of large spread in Arctic freshwater storage simulated in CMIP5 models (Shu et al., 2018) remains in the CMIP6 models.

In summary, the CMIP6 MMM shows strong warming in the Arctic AW layer and at the surface for both future scenarios considered in this study. The AW layer will become shallower. The warming in the bulk of the AW layer causes the temperature climate change in the Arctic deep basins to be much larger than the global mean change. The Arctic halocline will become much fresher in the future, in particular in the Canadian Basin. However, the CMIP6 models have large spread in the simulated climate change signals for both temperature and salinity.

4 Discussion

Most of the state-of-the-art CMIP6 models simulate a warm AW layer below the cold halocline in the Arctic Ocean, which is one of the key characteristics of the Arctic ocean evident from observations However, this AW layer is too thick and too deep compared to observations in most of the CMIP6 models and also in the MMM. This issue has been found in forced ocean simulations more than a decade ago (Holloway et al., 2007); it was prevalent in both forced and coupled ocean simulations in the period of CMIP5

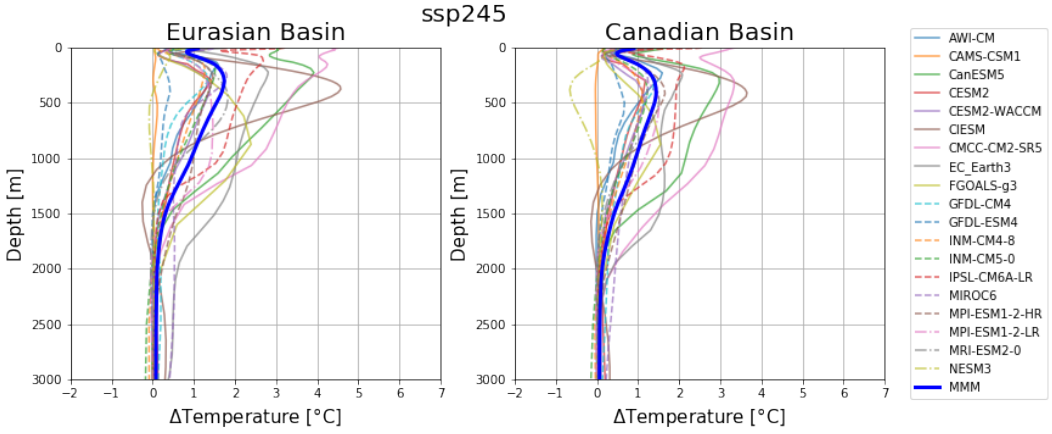

(a)

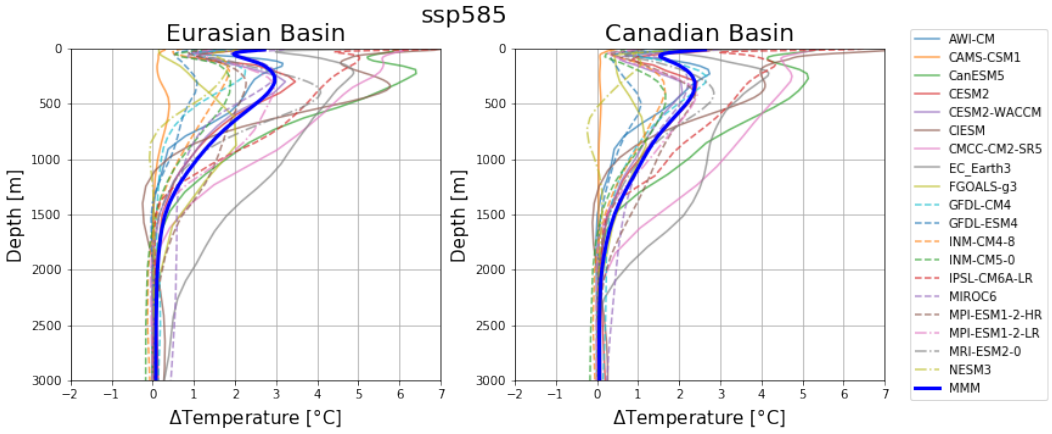

(b)

Figure 4: Projected climate change in potential temperature for the Eurasian (left) and Canadian (right) basins based on two CMIP6 scenarios: SSP245 (top) and SSP585 (bottom). Climate change is defined as the difference between the periods 2081-2100 and 1995-2014.

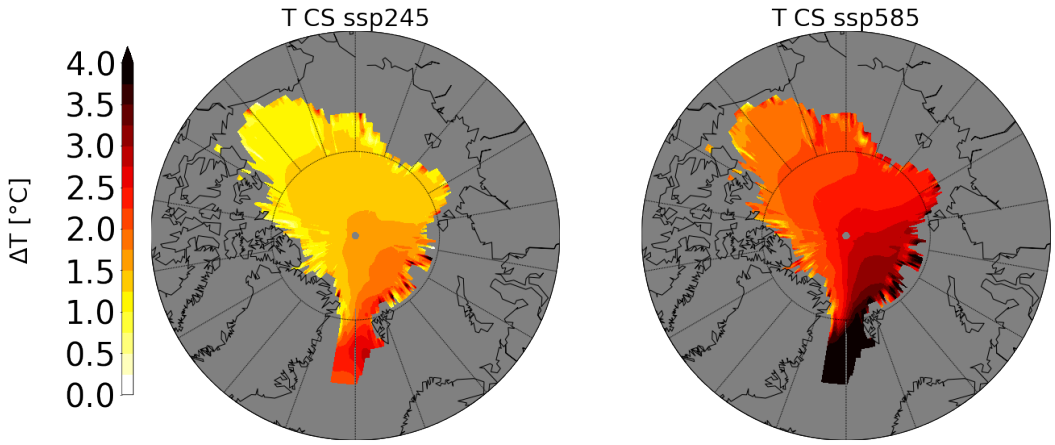

Figure 5: Projected climate change of the Atlantic Water core temperature (AWCT) for the Arctic deep basin generated using two CMIP6 scenarios: SSP245 (left) and SSP585 (right). Climate change is defined as the difference between the periods 2081-2100 and 1995-2014.

(Ilıcak et al., 2016; Shu et al., 2019), and it continues to remain a critical issue in CMIP6 models, as shown by our analysis. There is agreement across the above-mentioned studies that numerical mixing in coarse resolution models is a main reason for this issue. Indeed, it was found that increasing horizontal resolution to 4.5 km in the Arctic Ocean, although not fully eddy resolving yet, can significantly reduce the too thick and too deep biases of the AW layer (Wang et al., 2018). The CMIP6 models on average have a too fresh mid to lower halocline, as in CMIP5 models (Shu et al., 2019), which means a weaker stratification in the associated depth range. Strong diapycnal mixing can weaken the halocline stratification (Zhang & Steele, 2007). So it is very possible that the diapycnal numerical mixing associated with coarse model resolution is partially responsible for the salinity bias too.

The horizontal resolution in CMIP6 models can be still considered coarse (Table 1), and much coarser than the resolution of 4.5 km that was found to be very effective in reducing long-standing model biases (Wang et al., 2018). Even in the HighResMIP of CMIP6, the high resolution in the Arctic Ocean is only 1/4 degree (Docquier et al., 2019). Nevertheless, these models can improve the AW heat transport toward the Arctic Ocean to some extent in comparison to the models using 1 degree resolution – thus encouraging the use of higher model resolution in future CMIP efforts. There is ongoing effort to reduce numerical mixing through improving model formulations (Griffies et al., 2020). As the model biases discussed above are very possibly associated with numerical mixing in the models, it remains to be seen whether such improvement can make a breakthrough change in model performance in the Arctic Ocean in next generations of CMIP simulations.

As shown in Section 3.1, the CMIP6 models have a large spread in the simulated AWCT and most of them have large negative or positive biases in the AWCT in historical simulations (Figure 1a and Figure 2a). In this context, it is interesting to understand whether the realism of models in simulating present day climate is related to how they project future changes. That is, do models with large positive biases have stronger warming in the future scenarios, and vice versa? The relationship of Arctic-mean AWCT in the present day period and its climate change signals (that is, the AWCT change between present day and long-term future) is shown in Figure 8. Their correlation coefficients are

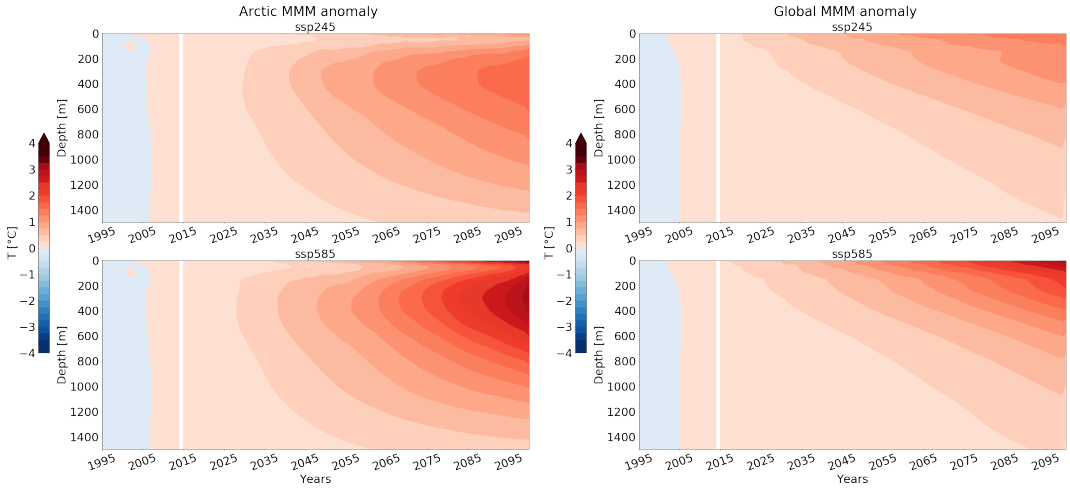

(a)

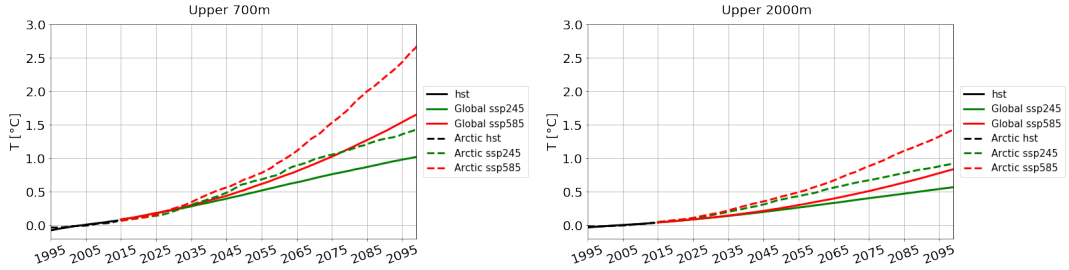

(b)

Figure 6: (a) Hovmöller diagrams of temperature anomalies (depth vs. time) for the Arctic Ocean (left) and global ocean (right). Only ocean areas with bottom bathymetry deeper than 300 m are considered. (b) Time series of temperature anomalies averaged over the upper 700 m (left) and 2000 m (right). Temperature anomalies are relative to the average over the present day (1995-2014) period. The same plots but for all ocean areas (without excluding shelf regions with topography shallower than 300 m) are shown in Figure S5. The difference from this figure is negligible.

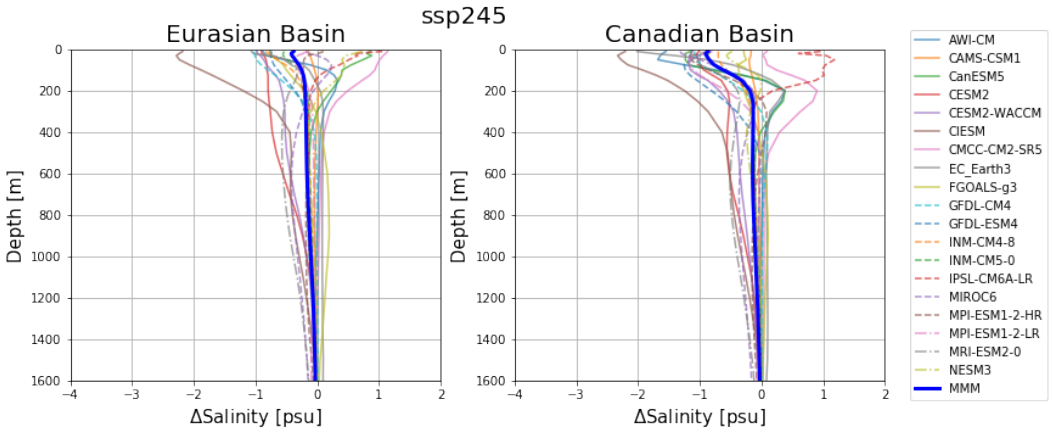

(a)

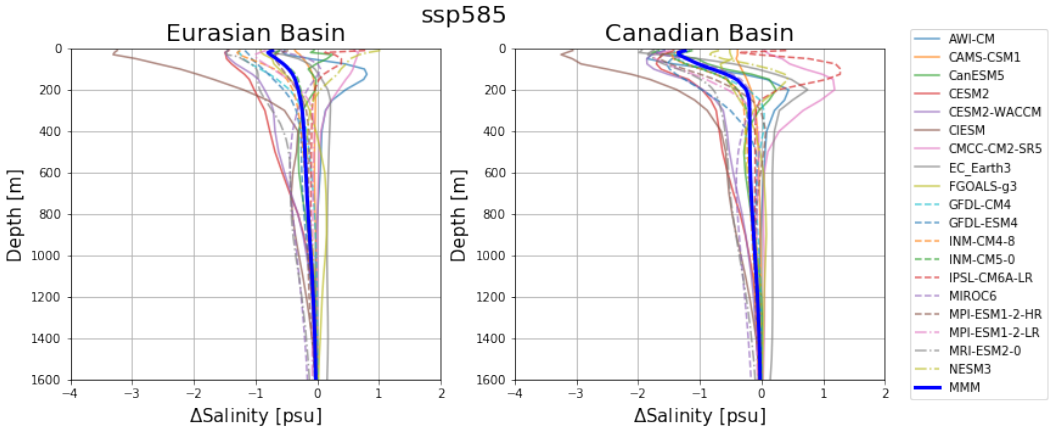

(b)

Figure 7: The salinity climate change signals for Eurasian and Canadian basins in CMIP6 projections ssp245 (top) and ssp585 (bottom). The climate change signal is defined as the difference between two periods (2081-2100 minus 1995-2014) according to IPCC AR6.

relatively low in both basins for the SSP245 scenario, and even lower for the SSP585 scenario, regardless of whether the "outlier models" are considered or not. The results indicate that the projected future AWCT changes are statistically independent of the model biases in present day simulations in the SSP585 scenario. In the SSP245 scenario, the AWCT climate change signals are weakly and negatively correlated with the present day AWCT, indicating that the AW warming tends to be slightly weaker in models with larger positive AWCT biases. However, the observed present day AWCT (0.5-1°C) is at the center of the AWCT range of the model simulations, so the impact of model biases on the predicted climate change signals in individual models, if any, does not significantly influence the predicted MMM climate change signals. Note that the present day AWCT is strongly correlated with the long-term future AWCT (Figure S7), simply because the range of climate change signals is not larger than the range of the present day AWCT among the models. Physically, it means that models that overestimate (underestimate) present day AWCT tend to have higher (lower) AWCT in the future, although this is not the case for all models, like those outlier models indicated in Figure 8 and Figure S7.

As mentioned in Section 3.2, CMIP6 models suggest that the Arctic deep basins will warm up more strongly than the global ocean on average. An interesting follow-up question is how the warming in the Arctic compares to the individual ocean basins in the world ocean. The spatial patterns of projected climate change for the temperature averaged over the upper 700 m reveal warming hotspots and warming holes, which are consistent between the two scenarios (Figure 9). The most outstanding warming holes include the southern part of the Southern Ocean and the North Atlantic subpolar gyre (consistent with previous findings, e.g, (Sévellec et al., 2017; Hu & Fedorov, 2020; Keil et al., 2020)), while the hotspots can be found mainly on the Northern Hemisphere except for part of the northern band of the Southern Ocean, including the western coasts and western boundary currents in both North Atlantic and North Pacific, the northern Nordic Seas, the Barents Sea, and the eastern Bering Sea. Importantly, the sub-Arctic seas close to the entrance of inflows to the Arctic Ocean are all warming hotspots, namely the northern Nordic Sea, the Barents Sea and the Bering Sea. As the climate change signals of ocean surface temperature are quite close in the Eurasian and Canadian Basin (Figure 4), the warming in the Pacific Water inflow, which mainly enters the upper Arctic Ocean, does not have a significant contribution to the warming in the deep basin areas. On the contrary, the warming in the Atlantic Water inflow supplies the significant warming in the Arctic AW layer (Figure 5). Although the Arctic deep basins will not warm up as strongly as at the warming hotspots mentioned above, the warming in the Eurasian Basin will be at least as strong as in the North Atlantic subtropical gyre and North Pacific subpolar gyre. Even in the Canadian Basin, which has weaker warming than in the Eurasian Basin, the warming will be much stronger than in the warming holes and slightly stronger than in Indian Ocean and the equatorial and south Pacific in both scenarios.

The MMM shows that the upper ocean including the upper halocline and mixed layer will become fresher in a warming climate (Figure 7), while, simultaneously, the AW layer will become warmer and the AWCD will become shallower (Figure 4 and Figure S3). The uplift and warming of the AW layer implies that winter convection, if it happens, does not need to reach very deep to bring up ocean heat. This will be especially true in the Eurasian Basin, because the decrease in upper ocean salinity, thus the increase in stratification, is much smaller in the Eurasian Basin than in the Canadian Basin in the MMM (Figure 7). However, the models have large spread in the projected salinity and temperature changes in both scenarios. Some models obtain salinification in the upper ocean, thus weakening in the ocean stratification, while some models obtain upper ocean freshening that is much stronger than the MMM, thus a significant increase in the ocean stratification (Figure 7). Therefore, the models do not agree on changes in the strength of vertical mixing and the possibility of emergence of deep convection in the Arctic deep

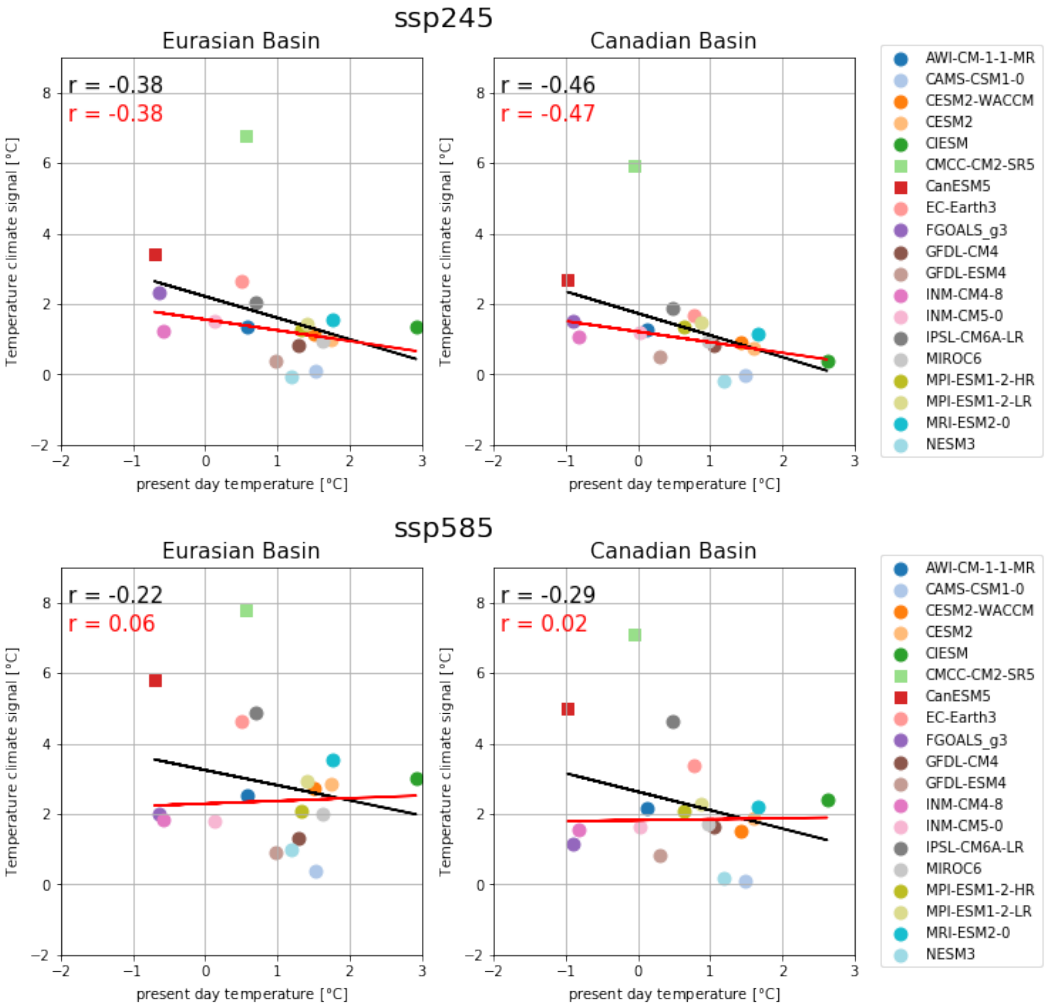

Figure 8: The climate change signals of Atlantic Water Core Temperature (AWCT) vs. the present day AWCT. The results for the Eurasian and Canadian basins and two scenarios are shown. Linear fits and correlation coefficients are also indicated in the plots (black color). Two models with AWCT climate change signals significantly different from others in at least one of the scenarios, are shown by squares instead of circles. These models are also excluded to calculate the correlation coefficients and regression lines (red color).

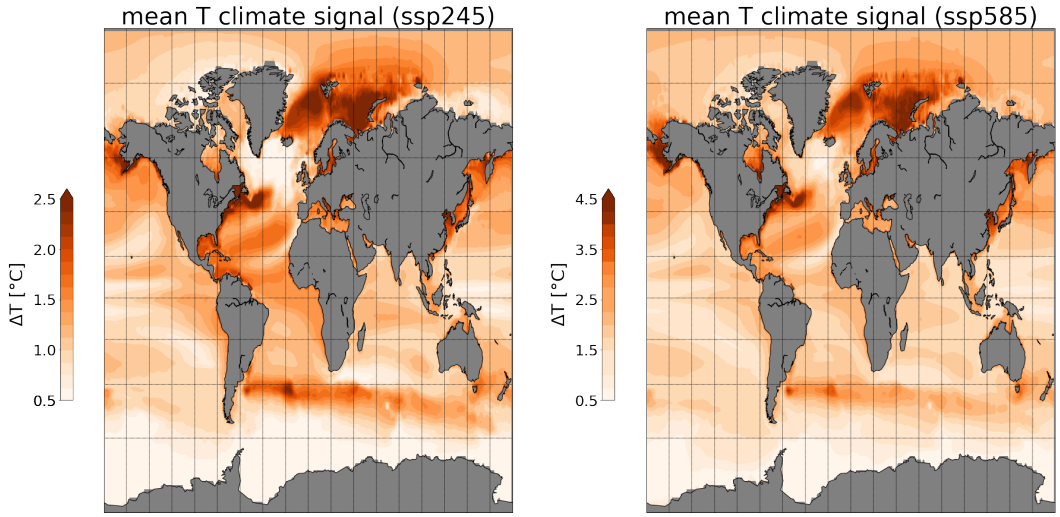

Figure 9: Climate change of temperature averaged over upper 700 m in the SSP245 (left) and SSP585 (right) scenarios. Climate change is defined as the difference between the periods 2081-2100 and 1995-2014

basin as well. In order to predict the future development of the Arctic Atlantification and its possible impact on sea ice, model uncertainties need to be considerably reduced. As some of the model biases identified in this paper could have origins outside the Arctic Ocean and possibly in other components of the climate system, major efforts to systematically reduce model uncertainties in the future CMIP simulations are required.

5 Conclusion

In this study, we assessed the temperature and salinity in the Arctic deep basin (the Eurasian and Canadian basins) in CMIP6 historical simulations and the respective climate change signals in the SSP245 and SSP585 scenarios. One of our main findings is that the biases in Arctic Ocean temperature and salinity found in CMIP5 historical simulations remain virtually unchanged in the CMIP6 simulations. The Atlantic Water (AW) layer is still too deep and too thick in nearly all models, the multi-model-mean (MMM) halocline is too fresh, and the models have a large spread in both the simulated temperature and salinity. Even some details in model biases in CMIP6 models are also very similar to those in CMIP5 models. Therefore, it can be concluded that there is essentially no improvement in the representation of the hydrography in the Arctic deep basins from CMIP5 to CMIP6.

Both the Arctic AW layer and upper ocean are projected to become warmer in the future as indicated by the CMIP6 MMM. The warming in the Arctic deep basins in the long-term future (2081-2100) relative to the present day conditions (1995-2014) is the largest in the upper AW layer (200-500 m) for MMM, with a magnitude of about 1.7°C and 1.4°C in the Eurasian and Canadian basins in SSP245, respectively, and about 3°C and 2.4°C in SSP585. The warming in the upper AW layer results in an uplift of the AW layer. The climate change signal of ocean surface temperature in the areas of Arctic deep basins in the MMM is about 1°C and 2.8°C in the SSP245 and SSP585 scenarios, respectively. In the depth range of the Arctic AW layer, the Arctic Ocean has a stronger warming trend than the global mean. Averaged over the upper 700 m, the increase in Arctic basin temperature at the end of the 21st century is 40% and 60% higher than the global mean in the SSP245 and SSP585 scenarios, respectively. The warming in the Arctic Ocean

is even stronger than that in most of the world ocean basins on average. We further found that all the sub-Arctic seas close to the Arctic inflow gateways are warming hotspots in a warming climate, including the northern Nordic Seas, Barents Sea and eastern Bering Sea. In particular, the strong warming in the AW inflow supplies the warming of the Arctic AW layer. The warming trend in the AW inflow is not only induced by warming upstream in the North Atlantic, but also can be enhanced by local atmospheric warming around the Arctic gateways (e.g., (Asbjørnsen et al., 2020) and feedback processes (e.g. (Wang et al., 2020)).

We also explored the relationship between the simulated present day AW core temperature (AWCT, the maximum temperature in the AW layer at each location) averaged over the Arctic Ocean and its climate change signals (the extent of the future warming). We found that the climate change signal of AWCT is not sensitive to the biases in the present day simulations, especially in the SSP585 scenario. In the SSP245 scenario, the climate change signals are weakly correlated with the model biases. However, considering that the simulated present day AWCT in the CMIP6 models is distributed around the observation, the MMM climate change signal is not subjected to significant corrections using the found correlation relationship.

The MMM upper ocean salinity is found to decrease in both Arctic basins in the future scenarios, with the decrease in the Canadian Basin being stronger than in the Eurasian Basin. Therefore, the stratification in the Arctic upper ocean is projected to be more stable in the MMM in both the SSP245 and SSP585 scenarios. However, the models have a large spread in the simulated climate change for upper ocean salinity, with some models having upper ocean salinification and some having upper ocean freshening. The upper ocean stratification influences the strength of vertical mixing, thus the impact of AW layer on sea ice, so the CMIP6 models do not agree on the extent to which the future changes in AW layer may influence the sea ice. The identified model biases with a wide spread in the simulated temperature and salinity in the CMIP6 models reported in this paper call for a collective effort to systematically improve coupled model simulations in future CMIP models.

Acknowledgments

The work described in this paper has received funding from the European Union's Horizon 2020 Research Innovation programme through grant agreement No. 727862 APPLICATE. The content of the paper is the sole responsibility of the authors and it does not represent the opinion of the European Commission, and the Commission is not responsible for any use that might be made of the information contained. This work is also supported by the German Helmholtz Climate Initiative REKLIM (Regional Climate Change). This paper is a contribution to the projects S1 (Diagnosis and Metrics in Climate Models) and S2 (Improved parameterizations and numerics in climate models) of the Collaborative Research Centre TRR 181 "Energy Transfer in Atmosphere and Ocean" funded by the Deutsche Forschungsgemeinschaft (DFG, German Research Foundation) – project no. 274762653. The CMIP6 data were downloaded from `https://esgf-data.dkrz.de/projects/esgf-dkrz/` and PHC3 data from `http://psc.apl.washington.edu/nonwp_projects/PHC/Data3.html`

References

Asbjørnsen, H., Årthun, M., Skagseth, Ø., & Eldevik, T. (2020). Mechanisms underlying recent arctic atlantification. *Geophysical Research Letters*, *47*(15), e2020GL088036.

Canuto, V., Howard, A., Cheng, Y., & Dubovikov, M. (2001). Ocean turbulence. part i: One-point closure model—momentum and heat vertical diffusivities. *Journal of Physical Oceanography*, *31*(6), 1413–1426.

Canuto, V., Howard, A., Cheng, Y., & Dubovikov, M. (2002). Ocean turbulence. part ii: Vertical diffusivities of momentum, heat, salt, mass, and passive scalars. *Journal of Physical Oceanography*, *32*(1), 240–264.

Carmack, E., Polyakov, I., Padman, L., Fer, I., Hunke, E., Hutchings, J., ... others (2015). Toward quantifying the increasing role of oceanic heat in sea ice loss in the new arctic. *Bulletin of the American Meteorological Society*, *96*(12), 2079–2105.

Dai, A., Luo, D., Song, M., & Liu, J. (2019). Arctic amplification is caused by sea-ice loss under increasing co 2. *Nature communications*, *10*(1), 121.

Dmitrenko, I. A., Kirillov, S. A., Serra, N., Koldunov, N., Ivanov, V. V., Schauer, U., ... others (2014). Heat loss from the atlantic water layer in the northern kara sea: Causes and consequences. *Ocean Science*, *10*(4), 719–730.

Dmitrenko, I. A., Polyakov, I. V., Kirillov, S. A., Timokhov, L. A., Frolov, I. E., Sokolov, V. T., ... Walsh, D. (2008). Toward a warmer arctic ocean: Spreading of the early 21st century atlantic water warm anomaly along the eurasian basin margins. *Journal of Geophysical Research: Oceans*, *113*(C5).

Docquier, D., Grist, J. P., Roberts, M. J., Roberts, C. D., Semmler, T., Ponsoni, L., ... others (2019). Impact of model resolution on arctic sea ice and north atlantic ocean heat transport. *Climate Dynamics*, *53*(7-8), 4989–5017.

Eyring, V., Bony, S., Meehl, G. A., Senior, C. A., Stevens, B., Stouffer, R. J., & Taylor, K. E. (2016). Overview of the coupled model intercomparison project phase 6 (cmip6) experimental design and organization. *Geoscientific Model Development (Online)*, *9*(LLNL-JRNL-736881).

Gaspar, P., Grégoris, Y., & Lefevre, J.-M. (1990). A simple eddy kinetic energy model for simulations of the oceanic vertical mixing: Tests at station papa and long-term upper ocean study site. *Journal of Geophysical Research: Oceans*, *95*(C9), 16179–16193.

Giles, K. A., Laxon, S. W., Ridout, A. L., Wingham, D. J., & Bacon, S. (2012). Western arctic ocean freshwater storage increased by wind-driven spin-up of the beaufort gyre. *Nature Geoscience*, *5*(3), 194–197.

Griffies, S. M., Adcroft, A., & Hallberg, R. W. (2020). A primer on the vertical lagrangian-remap method in ocean models based on finite volume generalized vertical coordinates. *Journal of Advances in Modeling Earth Systems*, *12*(10), e2019MS001954.

Hattermann, T., Isachsen, P. E., von Appen, W.-J., Albretsen, J., & Sundfjord, A. (2016). Eddy-driven recirculation of atlantic water in fram strait. *Geophysical Research Letters*, *43*(7), 3406–3414.

Holloway, G., Dupont, F., Golubeva, E., Häkkinen, S., Hunke, E., Jin, M., ... others (2007). Water properties and circulation in arctic ocean models. *Journal of Geophysical Research: Oceans*, *112*(C4).

Hu, S., & Fedorov, A. V. (2020). Indian ocean warming as a driver of the north atlantic warming hole. *Nature communications*, *11*(1), 1–11.

Ilıcak, M., Drange, H., Wang, Q., Gerdes, R., Aksenov, Y., Bailey, D., ... others (2016). An assessment of the arctic ocean in a suite of interannual core-ii simulations. part iii: Hydrography and fluxes. *Ocean Modelling*, *100*, 141–161.

Ivanov, V., Alexeev, V., Koldunov, N. V., Repina, I., Sandø, A. B., Smedsrud, L. H., & Smirnov, A. (2016). Arctic ocean heat impact on regional ice decay: A suggested positive feedback. *Journal of Physical Oceanography*, *46*(5), 1437–1456.

Johannessen, O. M., Bengtsson, L., Miles, M. W., Kuzmina, S. I., Semenov, V. A., Alekseev, G. V., ... others (2004). Arctic climate change: observed and modelled temperature and sea-ice variability. *Tellus A: Dynamic meteorology and oceanography*, *56*(4), 328–341.

Keil, P., Mauritsen, T., Jungclaus, J., Hedemann, C., Olonscheck, D., & Ghosh, R. (2020). Multiple drivers of the north atlantic warming hole. *Nature Climate Change*, *10*(7), 667–671.

Large, W. G., McWilliams, J. C., & Doney, S. C. (1994). Oceanic vertical mixing: A review and a model with a nonlocal boundary layer parameterization. *Reviews of Geophysics*, *32*(4), 363–403.

Marnela, M., Rudels, B., Houssais, M.-N., Beszczynska-Möller, A., Eriksson, P., et al. (2013). Recirculation in the fram strait and transports of water in and north of the fram strait derived from ctd data. *Ocean Science*.

Meehl, G. A., Boer, G. J., Covey, C., Latif, M., & Stouffer, R. J. (2000). The coupled model intercomparison project (cmip). *Bulletin of the American Meteorological Society*, *81*(2), 313–318.

Noh, Y., & Jin Kim, H. (1999). Simulations of temperature and turbulence structure of the oceanic boundary layer with the improved near-surface process. *Journal of Geophysical Research: Oceans*, *104*(C7), 15621–15634.

Notz, D., & Stroeve, J. (2016). Observed arctic sea-ice loss directly follows anthropogenic co2 emission. *Science*, *354*(6313), 747–750.

O'Neill, B. C., Tebaldi, C., Vuuren, D. P. v., Eyring, V., Friedlingstein, P., Hurtt, G., ... others (2016). The scenario model intercomparison project (scenariomip) for cmip6. *Geoscientific Model Development*, *9*(9), 3461–3482.

Pacanowski, R., & Philander, S. (1981). Parameterization of vertical mixing in numerical models of tropical oceans. *Journal of Physical Oceanography*, *11*(11), 1443–1451.

Polyakov, I. V., Beszczynska, A., Carmack, E. C., Dmitrenko, I. A., Fahrbach, E., Frolov, I. E., ... others (2005). One more step toward a warmer arctic. *Geophysical Research Letters*, *32*(17).

Polyakov, I. V., Pnyushkov, A. V., Alkire, M. B., Ashik, I. M., Baumann, T. M., Carmack, E. C., ... others (2017). Greater role for atlantic inflows on sea-ice loss in the eurasian basin of the arctic ocean. *Science*, *356*(6335), 285–291.

Polyakov, I. V., Timokhov, L. A., Alexeev, V. A., Bacon, S., Dmitrenko, I. A., Fortier, L., ... others (2010). Arctic ocean warming contributes to reduced polar ice cap. *Journal of Physical Oceanography*, *40*(12), 2743–2756.

Proshutinsky, A., & Kowalik, Z. (2007). Preface to special section on arctic ocean model intercomparison project (aomip) studies and results. *Journal of Geophysical Research: Oceans*, *112*(C4).

Proshutinsky, A., Krishfield, R., Toole, J., Timmermans, M.-L., Williams, W., Zimmermann, S., ... others (2019). Analysis of the beaufort gyre freshwater content in 2003–2018. *Journal of Geophysical Research: Oceans*, *124*(12), 9658–9689.

Proshutinsky, A., Steele, M., & Timmermans, M.-L. (2016). Forum for arctic modeling and observational synthesis (famos): Past, current, and future activities. *Journal of Geophysical Research: Oceans*, *121*(6), 3803–3819.

Reichl, B. G., & Hallberg, R. (2018). A simplified energetics based planetary boundary layer (epbl) approach for ocean climate simulations. *Ocean Modelling*, *132*, 112–129.

Rudels, B., & Friedrich, H. J. (2000). The transformations of atlantic water in the arctic ocean and their significance for the freshwater budget. In *The freshwater budget of the arctic ocean* (pp. 503–532). Springer.

Schauer, U., Beszczynska-Möller, A., Walczowski, W., Fahrbach, E., Piechura, J., & Hansen, E. (2008). Variation of measured heat flow through the fram strait between 1997 and 2006. In *Arctic–subarctic ocean fluxes* (pp. 65–85). Springer.

Schulzweida, U. (2019). *Cdo user guide (version 1.9. 6)*.

Serreze, M. C., & Francis, J. A. (2006). The arctic amplification debate. *Climatic change*, *76*(3-4), 241–264.

Serreze, M. C., & Stroeve, J. (2015). Arctic sea ice trends, variability and implications for seasonal ice forecasting. *Philosophical Transactions of the Royal Society A: Mathematical, Physical and Engineering Sciences*, *373*(2045),

20140159.

Sévellec, F., Fedorov, A. V., & Liu, W. (2017). Arctic sea-ice decline weakens the atlantic meridional overturning circulation. *Nature Climate Change*, *7*(8), 604–610.

Shu, Q., Qiao, F., Song, Z., Zhao, J., & Li, X. (2018). Projected freshening of the arctic ocean in the 21st century. *Journal of Geophysical Research: Oceans*, *123*(12), 9232–9244.

Shu, Q., Wang, Q., Su, J., Li, X., & Qiao, F. (2019). Assessment of the atlantic water layer in the arctic ocean in cmip5 climate models. *Climate Dynamics*, *53*(9-10), 5279–5291.

Smedsrud, L. H., Esau, I., Ingvaldsen, R. B., Eldevik, T., Haugan, P. M., Li, C., ... others (2013). The role of the barents sea in the arctic climate system. *Reviews of Geophysics*, *51*(3), 415–449.

Steele, M., Morley, R., & Ermold, W. (2001). Phc: A global ocean hydrography with a high-quality arctic ocean. *Journal of Climate*, *14*(9), 2079–2087.

Umlauf, L., & Burchard, H. (2003). A generic length-scale equation for geophysical turbulence models. *Journal of Marine Research*, *61*(2), 235–265.

Wang, Q., Ilicak, M., Gerdes, R., Drange, H., Aksenov, Y., Bailey, D. A., ... others (2016a). An assessment of the arctic ocean in a suite of interannual core-ii simulations. part ii: Liquid freshwater. *Ocean Modelling*, *99*, 86–109.

Wang, Q., Ilicak, M., Gerdes, R., Drange, H., Aksenov, Y., Bailey, D. A., ... others (2016b). An assessment of the arctic ocean in a suite of interannual core-ii simulations. part i: Sea ice and solid freshwater. *Ocean Modelling*, *99*, 110–132.

Wang, Q., Wekerle, C., Danilov, S., Sidorenko, D., Koldunov, N., Sein, D., ... Jung, T. (2019). Recent sea ice decline did not significantly increase the total liquid freshwater content of the arctic ocean. *Journal of Climate*, *32*(1), 15–32.

Wang, Q., Wekerle, C., Danilov, S., Wang, X., & Jung, T. (2018). A 4.5 km resolution arctic ocean simulation with the global multi-resolution model fesom1. 4. *Geosci. Model Dev.*, *11*, 1229–1255.

Wang, Q., Wekerle, C., Wang, X., Danilov, S., Koldunov, N., Sein, D., ... Jung, T. (2020). Intensification of the atlantic water supply to the arctic ocean through fram strait induced by arctic sea ice decline. *Geophysical Research Letters*, *47*(3), e2019GL086682.

Wekerle, C., Wang, Q., von Appen, W.-J., Danilov, S., Schourup-Kristensen, V., & Jung, T. (2017). Eddy-resolving simulation of the atlantic water circulation in the fram strait with focus on the seasonal cycle. *Journal of Geophysical Research: Oceans*, *122*(11), 8385–8405.

Zhang, J., & Steele, M. (2007). Effect of vertical mixing on the atlantic water layer circulation in the arctic ocean. *Journal of geophysical research: Oceans*, *112*(C4).